THEORETICAL PREDICTIONS AND EXPERIMENTAL MEASUREMENTS OF ECHO RESPONSES FROM TILTED FLAT-BOTTOMED HOLES

Alain Lhémery *
École Centrale Paris, Laboratoire de Mécanique, URA 850 C.N.R.S.
Grande Voie des Vignes, 92295 Châtenay-Malabry *cedex*, France

John P. Weight
The City University, Dpt. of EEIE, Northampton Square, EC1V0HB
London, United Kingdom

INTRODUCTION

In some earlier work, semi-analytic methods were proposed to predict echo responses from point-like targets [1] and normally aligned flat-bottomed holes in solids (FBH) [2]. A new, more general formulation has recently been developed (hereafter, the "*elastic* model" [3]), capable of predicting responses from defects of arbitrary shape. In this paper, theoretical predictions using the new model are compared with experimentally measured echo responses from tilted FBH's, where the hole bottom is tilted relative to the transducer axis. A related study [4] has already been presented in which experimental echo responses from tilted disks immersed in a fluid were compared with results predicted by an earlier model [5]. In that earlier model, mode conversion was not taken into account and only compression waves were considered (the "*acoustic* model").

The *acoustic* and *elastic* models take account of transducer diffraction effects (both in radiation and reception). In both models, the mechanical impulse response of the whole problem of radiation, scattering by defect and reception are computed. Note that these impulse responses are independent of any electo-acoustical phenomena. A knowledge of the impulse response of defects gives great insight into the complex echo structure arising from the geometry considered. The comparison [3] of both *acoustic* and *elastic* impulse responses leads to an interpretation of results in terms of geometrical and mode converted contributions.

In the first section, the new *elastic* model is reviewed. The second section describes the experimental setup and shows the experimental validation of the *elastic* model. In conclusion, we discuss the usefulness of the new model in the context of its application for modeling nondestructive testing configurations.

* present address : Commissariat à l'Énergie Atomique, DTA / CEREM / STA, CE-Saclay, Bat. 611, 91191 Gif-sur-Yvette *cedex*, France.

Review of Progress in Quantitative Nondestructive Evaluation, Vol. 15
Edited by D.O. Thompson and D.E. Chimenti, Plenum Press, New York, 1996

Transient radiation [6,7]

The model for calculating the field incident upon the defect predicts the transient displacement field radiated by an arbitrary source of traction $\mathbf{T}(\mathbf{r}_R,t)$ directly applied on the plane free surface of an elastic half-space, $\mathbf{r}_R$ being a running point of the radiating surface R. Space and time variables are assumed to be separable in the source term (piston source), so that $\mathbf{T}(\mathbf{r}_R,t) = \Gamma(\mathbf{r}_R)\, T(t)$. The i-th component of the displacement at a point $\mathbf{r}$ at time t is approximated by a sum of convolution integrals of displacement impulse-responses $\mathbf{h}(t)$ with $T(t)$.

$$u_i(\mathbf{r}, t) \approx T(t) * h_i(\mathbf{r}, t) = T(t) * [h_i^L(\mathbf{r}, t) + h_i^T(\mathbf{r}, t) + h_i^{T->L}(\mathbf{r},t)], \tag{1}$$

with,

$$h_i^L(\mathbf{r}, t) = \iint_R \frac{\gamma_i \gamma_j}{\lambda + 2\mu} \Gamma_j(\mathbf{r}_R) \frac{\delta(t - |\mathbf{r} - \mathbf{r}_R| / c_L)}{2\pi |\mathbf{r} - \mathbf{r}_R|} dS_R, \tag{2}$$

$$h_i^T(\mathbf{r}, t) = -\iint_R \frac{\gamma_i \gamma_j - \delta_{ij}}{\mu} \Gamma_j(\mathbf{r}_R) \frac{\delta(t - |\mathbf{r} - \mathbf{r}_R| / c_T)}{2\pi |\mathbf{r} - \mathbf{r}_R|} dS_R, \tag{3}$$

$$h_i^{T->L}(\mathbf{r}, t) = \int_{c_T}^{c_L} \iint_R \frac{3\,\gamma_i \gamma_j - \delta_{ij}}{\rho_0 c^2} \Gamma_j(\mathbf{r}_R) \frac{\delta(t - |\mathbf{r} - \mathbf{r}_R| / c)}{2\pi |\mathbf{r} - \mathbf{r}_R|} dS_R \frac{dc}{c}, \tag{4}$$

where $\gamma_i = (r_i - r_{R_i}) / |\mathbf{r} - \mathbf{r}_R|$, δ_{ij} is Kronecker's delta, ρ_0 denotes the density of the propagation medium and λ and μ (Lamé's coefficients) its elastic constants. c_L and c_T are the compression and shear wave velocities, given by $c_L = [(\lambda+2\mu)/\rho_0]^{1/2}$ and $c_T = (\mu/\rho_0)^{1/2}$.

Throughout, the summation convention for repeated subscripts is followed. In the case of a uniform disk thickness-mode transducer [$\mathbf{T}(\mathbf{r}_R,t) = \mathbf{1}_z\, T(t)$], the above integrals can be calculated analytically [6,7].

Scattering by a defect modeled as a free surface [2]

The scattering by a defect of insonified surface D is calculated under the Kirchhoff's approximation. In the case of a defect modeled as a traction free surface, the displacement field on the defect is proportionnal to the incident displacement,

$$u_i(\mathbf{r}_D,t) = \alpha(\mathbf{r}_D) u_i^{inc}(\mathbf{r}_D,t). \tag{5}$$

In Eq. (5) and in what follows, $\alpha(\mathbf{r})$ equals 0, 1 or 2 depending on whether $\mathbf{r}$ is outside, inside or on a locally smooth boundary of the propagation medium.

The resulting scattered field at an arbitrary point in the solid is expressed as,

$$u_n^{scat}(\mathbf{r},t) = -\int_{-\infty}^{+\infty} d\tau \iint_D \alpha(\mathbf{r}_D)\, u_i^{inc}(\mathbf{r}_D,\tau) c_{ijkl} n_j(\mathbf{r}_D) G_{kn,l}(\mathbf{r}_D, t-\tau; \mathbf{r}, 0) dS(\mathbf{r}_D), \tag{6}$$

where the third order Green tensor $G_{kn,l}$ is given by [8]

$$G_{ij,k}(\xi,\tau;\mathbf{r},t) = \frac{15\,\gamma_i\gamma_j\gamma_k - 3\gamma_i\delta_{jk} - 3\gamma_j\delta_{ik} - 3\gamma_k\delta_{ij}}{4\pi\rho_0}\,\frac{1}{r^4}\int_{r/c_L}^{r/c_T}\tau'\delta(t-\tau-\tau')\,d\tau'$$

$$+\frac{6\,\gamma_i\gamma_j\gamma_k - \gamma_i\delta_{jk} - \gamma_j\delta_{ik} - \gamma_k\delta_{ij}}{\rho_0 c_L^2}\,\frac{\delta(t-\tau-r/c_L)}{4\pi r^2} - \frac{6\,\gamma_i\gamma_j\gamma_k - \gamma_i\delta_{jk} - \gamma_j\delta_{ik} - 2\gamma_k\delta_{ij}}{\rho_0 c_T^2}\,\frac{\delta(t-\tau-r/c_T)}{4\pi r^2}$$

$$+\frac{\gamma_i\gamma_j\gamma_k}{\rho_0 c_L^3}\,\frac{\dot{\delta}(t-\tau-r/c_L)}{4\pi r} - \frac{\gamma_i\gamma_j\gamma_k - \gamma_k\delta_{ij}}{\rho_0 c_T^3}\,\frac{\dot{\delta}(t-\tau-r/c_T)}{4\pi r}\,. \qquad (7)$$

Reception by a transducer [1,3]

The transducer acting as a receiver is assumed to be sensitive to a combination of the various components of the particle velocity integrated over its active surface.

$$\langle v\rangle(t) \equiv \frac{\partial}{\partial t}\iint_R \Gamma_n(\mathbf{r}_R)\,u_n^{scat}(\mathbf{r}_R,t)\,dS_R\,. \qquad (8)$$

We can therefore easily define a reception impulse response independent of the rest of the propagation process as follows,

$$H_{k,l}(\mathbf{r}_D,t) = \iint_R \Gamma_n(\mathbf{r}_R)\,G_{kn,l}(\mathbf{r}_D,t\,;\,\mathbf{r}_R,0)dS_R\,, \qquad (9)$$

For transducer of simple symmetry and sensitivity distribution Γ, it is possible to calculate analytically the, in general nine (four in the case of axisymmetry) components of $H_{k,l}$.

Now, a simple combination of the above equations leads to the definition of an impulse response for the whole mechanical problem that links the time dependency of the source $T(t)$ to $\langle v\rangle(t)$ such that

$$\langle v\rangle(t) = H^{TSR}(t) * T(t) \qquad (10)$$

with

$$H^{TSR}(t) = -\frac{\partial}{\partial t}\iint_D [\,\alpha(\mathbf{r}_D)\,c_{ijkl}n_j(\mathbf{r}_D)h_i(\mathbf{r}_D,t) * H_{k,l}(\mathbf{r}_D,t)\,]\,dS_D\,. \qquad (11)$$

Application to tilted FBH's interrogated by a uniform disk thickness-mode transducer

The transducer works both as an emitter and a receiver. It is assumed to have uniform source and sensitivity distributions $\Gamma(r_R) = \mathbf{1}_z$ (over a circular area). The axisymmetry of the distribution allows one to calculate both the radiation and the reception impulse responses in cylindrical co-ordinates. The quantities to be calculated are h_r, h_z, $H_{r,r}$, $H_{z,z}$, $H_{r,z}$ and $H_{z,r}$. The defect (a FBH) being smooth, $\alpha(\mathbf{r}_D) = 2$ everywhere on the defect. Let θ be the tilt angle of the FBH (an angle $\theta = 0$ corresponds to the case of a normally aligned FBH). The convention of orientation of the vector surface $d\mathbf{S}_D$ leads to

$$n_r = \sin\theta \text{ and } n_z = \cos\theta . \quad (12)$$

In the case of an isotropic medium, the fourth order tensor of elastic constants is given by

$$c_{ijkl} = \lambda\, \delta_{ij}\, \delta_{kl} + \mu\, (\delta_{ik}\, \delta_{jl} + \delta_{il}\, \delta_{jk}) . \quad (13)$$

Let $H'_{rz} = H_{r,z} + H_{z,r}$, Taking account of Eq. (13), Eq. (11) for the tilted FBH becomes

$$H^{TSR}(t) = -\frac{\partial}{\partial t}\int_D\int \cos\theta\{h_z(\mathbf{r}_D,t) * [(\lambda+2\mu)H_{z,z}(\mathbf{r}_D,t)+\lambda H_{r,r}(\mathbf{r}_D,t)] + h_r(\mathbf{r}_D,t) * \mu H'_{rz}(\mathbf{r}_D,t)\}$$

$$+ \sin\theta\{h_r(\mathbf{r}_D,t) * [(\lambda+2\mu)H_{r,r}(\mathbf{r}_D,t)+\lambda H_{z,z}(\mathbf{r}_D,t)] + h_z(\mathbf{r}_D,t) * \mu H'_{rz}(\mathbf{r}_D,t)\}dS_D . \quad (14)$$

The complete analytic expressions of the radiation and reception impulse responses for a disk thickness mode transducer can be found in Ref. 3. They have been derived using the same approach as that used by Stepanishen [9] to obtain the exact calculation of the time dependent Rayleigh integral for a flat transducer radiating in a fluid medium.

COMPARISON OF PREDICTED AND MEASURED ECHO-RESPONSES

The elastic model may be used to calculate echo responses from defects insonified by pulses from arbitrary transducers. The transducer used in the experiments is a contact transducer and for experimental convenience and repeatability, a disk thickness-mode transducer was used, that is, a compression wave transducer.

In the present set of results we have concentrated on demonstrating how responses from targets vary with target tilt, and since such variation becomes stronger with target size, we have chosen to use target diameters that are greater than the (center frequency) interrogating pulse wavelength. To ensure a true simulation, the theoretical source driving function $T(t)$ used for the calculated results was set to match the plane-wave component of the pulse from the transducer used in making the experimental measurements. A convenient method to measure the radiated plane waveform is to record a backwall echo from a thin, parallel-sided plate: thin, since with increasing range the back wall echo becomes the derivative of $T(t)$ [1]. For the pulse shape and transducer diameter used here, a 10mm-thick plate was acceptable.

Experimental system

The targets considered were all flat-bottomed holes drilled at various angles into two aluminum test blocks (see Fig. 1). Two sets of holes of 4mm (tolerance +0.2mm) and 10mm (+0.5mm) diameter were machined. For each diameter there were 3 groups of 4 holes with depths chosen to give a metal path from the coupling surface to the center of the hole bottom of 12, 20 and 50mm (±0.5mm) respectively, each group including a hole inclined perpendicular to the coupling surface and 3 others at 5, 10 and 20 degrees (±0.5 degrees) respectively — making 24 test targets in all. The experimental measurements were made using a single, directly-coupled wideband transducer (Aerotech Alpha F08179 19mm diameter, 5 MHz) excited with a unidirectional pulse shaped to give an ultrasonic (plane wave) pulse of approximately one cycle at ~3MHz. In these preliminary measurements, all results were taken with the transducer positioned by hand to within ±1mm of the target axis, here defined as a line passing through the center of the hole bottom and perpendicular to the coupling surface. In later work we hope to devise a method to give better accuracy in transducer positioning. To guard against errors arising from variation in coupling conditions, repeated checks were

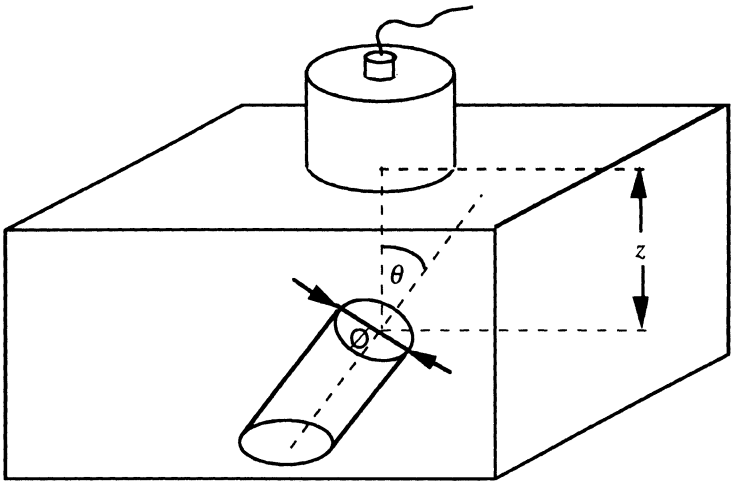

Fig. 1 Schematic view of a block used for the experiments.

made to monitor the reproducibility of a back-wall echo. The received echo responses were amplified by the wideband amplifier within a Panametrics 5052 PR pulser/receiver and recorded on a LeCroy 9410 digital oscilloscope.

Results

With the transducer/target geometry and the transducer pulse shape used here, the results for the smaller 4mm-diameter target given in Figure 2 shows some of the characteristics of the echo response of a point-like target [1], having a complicated multipulse structure arising from both diffraction effects and the existence of mode-converted shear waves. A full description of such a structure has been given elsewhere [1] but very briefly, the group of pulses labeled "C" denotes a packet of pulses with contributions due to the reception of scattered compression plane and edge waves; "C/S" is a packet that arises from the reception of waves that make one trip to/from the target as a compression wave and one as a shear wave and "S" shows a pulse that makes both trips as a shear wave. Bearing in mind the target machining tolerances and experimental errors in coupling and positioning the transducer, there is good agreement between the calculated and modelled results, excepting that the pulses labeled "M" are not seen in the theoretical results. These pulses are "multiple" echoes arising from that portion of the compression "C" packet that is reflected from the coupling surface to be further scattered by the target and then received back at the transducer. In its present form, the current model does not take such effects into account. Taking first the set of results for the targets at 12 mm range in Figure 2 we see that as is well known, the overall amplitude of the echo falls as the target is tilted from normal alignment (0°). Again, bearing in mind the experimental uncertainties, especially the error in transducer positioning, the model accurately predicts the changes in echo response shape and amplitude as the target is tilted. With increasing range, the time separation between the "C" and "CS" packets increases and the "S" pulse becomes too small to see at the scales used (for a fuller explanation of these effects see [1,3]). Note also that the drop in echo amplitude with angle of tilt increases with target range.

Figure 3 shows a similar set of results to those of Figure 2 but for the case of 10 mm diameter holes. Again with the exception of the multiples "M" that are stronger with these larger targets, there is good agreement between the measured and theoretical results. The

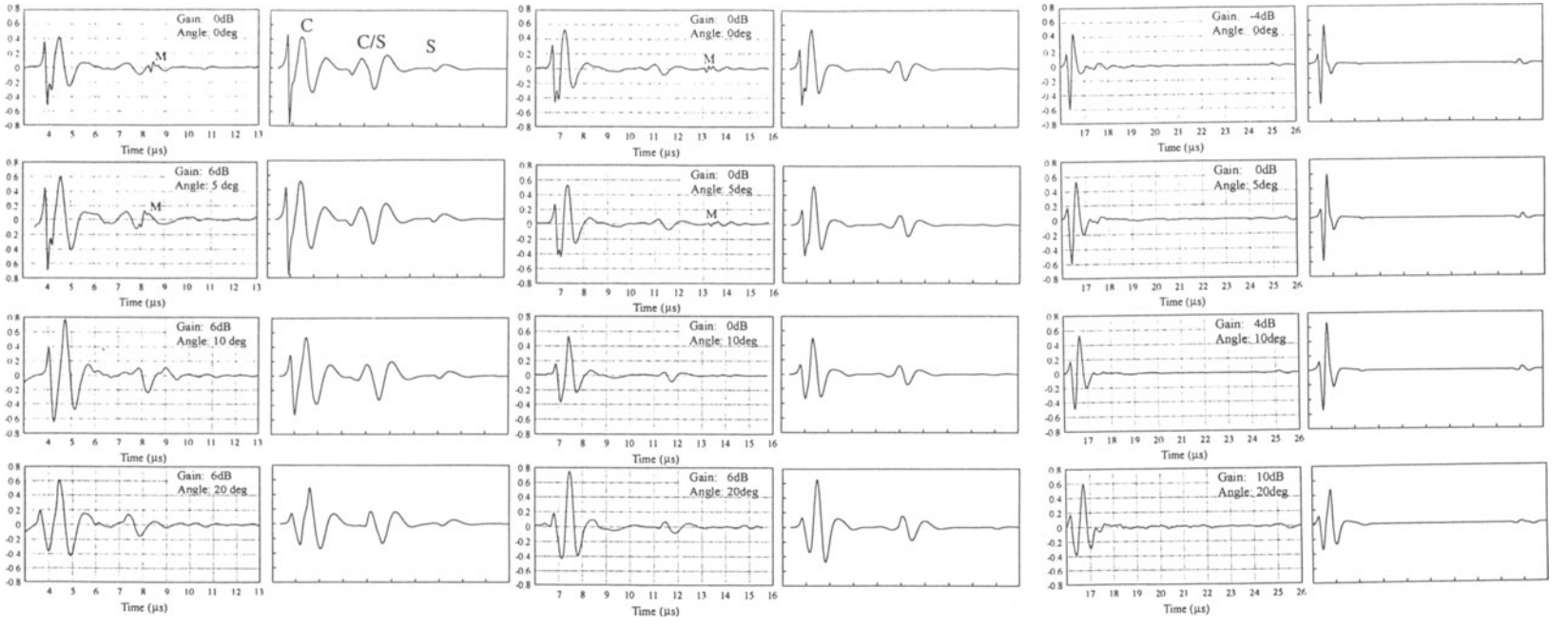

Fig. 2 Measured and calculated echo-responses from 4-mm-Ø tilted flat bottomed holes. First line : 0°; second 5°; third 10°; fourth 20° tilt angle. First (exp.) and second (calc.) column : 12-mm-range; third (exp.) and fourth (calc.) 20-mm, fifth (exp.) and sixth (calc.) 50-mm. (1 µs / div.). The measured and calculated waveforms are plotted to the same relative amplitude scales.

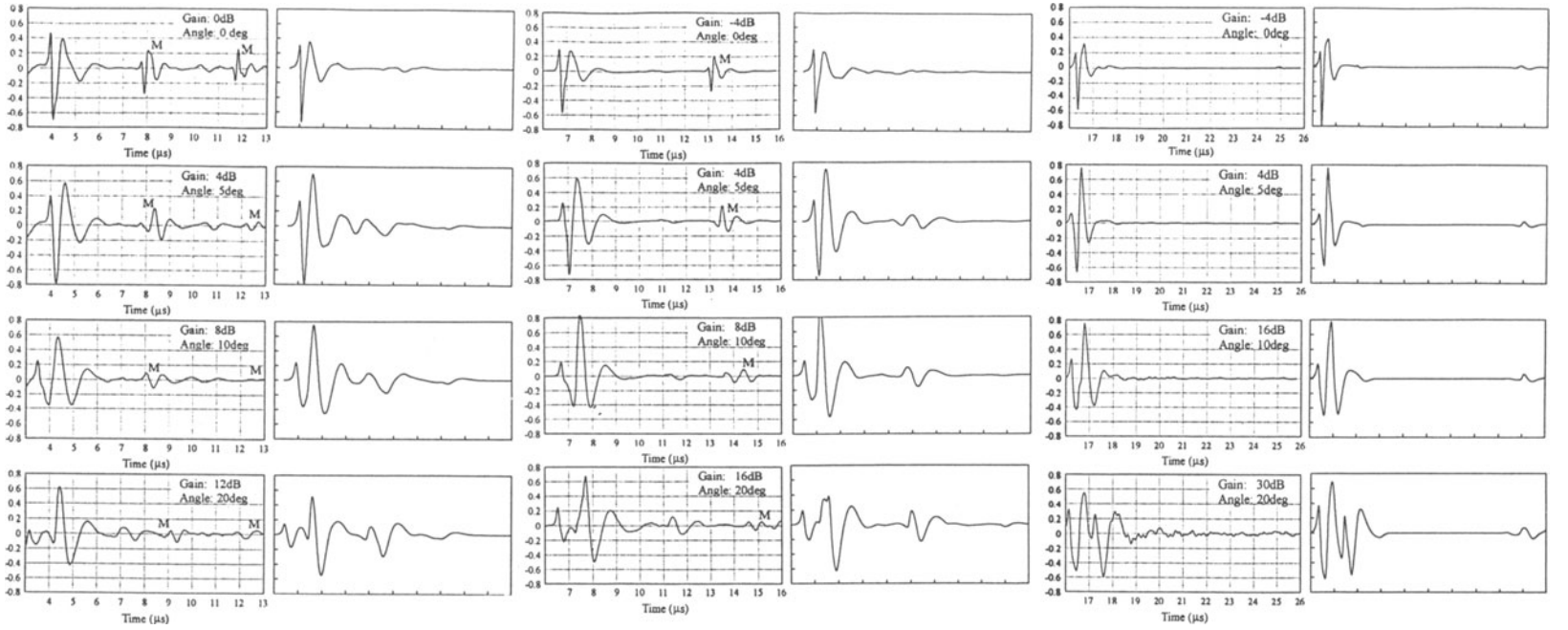

Fig. 3 Measured and calculated echo-responses from 10-mm-Ø tilted flat bottomed holes. First line : 0°; second 5°; third 10°; fourth 20° tilt angle. First (exp.) and second (calc.) column : 12-mm-range; third (exp.) and fourth (calc.) 20-mm, fifth (exp.) and sixth (calc.) 50-mm. (1 µs / div.). The measured and calculated waveforms are plotted to the same relative amplitude scales.

results for targets at normal alignment show that the first-arriving component of the overall response dominates over all later contributions. This is because when integrating over the surface of such targets it is only this first arriving component that has a constant time position, all other components being "smeared out" as the integration proceeds. As would be anticipated, the fall of in echo amplitude with angle of tilt is greater for the 10mm targets than is shown in Figure 2 for the smaller 4mm targets. With increasing angle of target tilt, the integrating effect mentioned above becomes less significant and it is possible to see a "CS" component in the responses from the targets at 10 and 20 degrees. Note also that at 20 degrees of tilt, the "C" component splits into two, from the nearer and further rims of the target, respectively. Such components are normally referred to as "diffracted pulses" and are made use of in target time-of-flight target sizing methods.

Taken together, the results of Figures 2 and 3 have great significance for the interpretation of echo responses. The existence of time-separated components in the overall responses can lead to the prediction of nonexistent targets and a knowledge of the origin of the later arriving "CS" and "S" pulses and the way in which their amplitude varies with target size, range and angular alignment can alleviate this. The ability to model the effects of various target geometry is of obvious benefit when attempting to size defects by relating their area to the amplitude of their echo response.

CONCLUSION

A new "*elastic* model" has been proved to give accurate predictions of echo responses from tilted flat-bottomed holes. The impulse response approach used gives a great insight into the complex echo structure arising from even the simple geometry considered here. The new model takes account of the existence of shear waves radiated from even a normally-coupled compression-wave transducer and includes some of the effects of mode conversion at the surface of the target, the target being considered as a free surface. In general, such a model is required to properly predict all of the components in the overall echo response, but with plane, normally-aligned targets that have dimensions of the order of a few (center frequency) wavelengths, or for arbitrarily sized targets in the far field, the simpler "acoustic" impulse response model can predict echo responses with reasonable accuracy. With small, near-field targets, the existence of mode-converted shear waves can give rise to time-separated echo pulses that could be confused as coming from nonexistent targets. Similar confusion could arise with larger near-field targets, except for the special case of a plane, normally-aligned target.

REFERENCES

1. J.P. Weight, J. Acoust. Soc. Am. 94, 514 (1993).
2. A. Lhémery, in *Review of Progress in QNDE*, Vol. 14, eds. D.O. Thompson and D.E. Chimenti (Plenum, New-York, 1994), p. 999.
3. A. Lhémery, J. Acoust. Soc. Am. 98 (1995).
4. A. Lhémery, J.P. Weight and R. Raillon, in *Review of Progress in QNDE*, Vol. 11, *op. cit.* (1992), p. 81.
5. A. Lhémery, J. Acoust. Soc. Am. 90, 2799 (1991).
6. A. Lhémery, J. Acoust. Soc. Am. 96, 3776 (1994).
7. A. Lhémery and R. Stacey, accepted for publication in the J. Acoust. Soc. Am. (1995).
8. K. Aki and P. G. Richard, *Quantitative seismology- Theory and experiments* (W.H. Freeman and Company, San Francisco, 1980), Ch. 2 - 3.
9. P.R. Stepanishen, J. Acoust. Soc. Am. 49, 1629 (1971).